



Research Article

Ginsenoside Rg5 promotes muscle regeneration via p38MAPK and Akt/mTOR signaling



Ryuni Kim ^{a,1}, Jee Won Kim ^{a,1}, Hyerim Choi ^a, Ji-Eun Oh ^b, Tae Hyun Kim ^a, Ga-Yeon Go ^{c,**}, Sang-Jin Lee ^{c,**}, Gyu-Un Bae ^{a,*}

^a Drug Information Research Institute, Muscle Physiome Research Center, College of Pharmacy, Sookmyung Women's University, Seoul, Republic of Korea

^b Department of Biomedical Laboratory Science, Far East University, Chungbuk-do, Republic of Korea

^c Research Institute of Aging Related Disease, AniMusCure Inc., Suwon, Republic of Korea

ARTICLE INFO

Article history:

Received 26 October 2022

Received in revised form

6 June 2023

Accepted 12 June 2023

Available online 24 June 2023

Keywords:

Ginsenoside

Glucocorticoids

Muscle atrophy

Myogenesis

Myotube growth

ABSTRACT

Background: Skeletal muscles play a key role in physical activity and energy metabolism. The loss of skeletal muscle mass can cause problems related to metabolism and physical activity. Studies are being conducted to prevent such diseases by increasing the mass and regeneration capacity of muscles. Ginsenoside Rg5 has been reported to exhibit a broad range of pharmacological activities. However, studies on the effects of Rg5 on muscle differentiation and growth are scarce.

Methods: To investigate the effects of Rg5 on myogenesis, C2C12 myoblasts were induced to differentiate with Rg5, followed by immunoblotting, immunostaining, and qRT-PCR for myogenic markers and pro-myogenic signaling (p38MAPK). Immunoprecipitation confirmed that Rg5 increased the interaction between MyoD and E2A via p38MAPK. To investigate the effects of Rg5 on prevention of muscle mass loss, C2C12 myotubes were treated with dexamethasone to induce muscle atrophy. Immunoblotting, immunostaining, and qRT-PCR were performed for myogenic markers, Akt/mTOR signaling for protein synthesis, and atrophy-related genes (Atrogin-1 and MuRF1).

Results: Rg5 promoted C2C12 myoblast differentiation through phosphorylation of p38MAPK and MyoD/E2A heterodimerization. Furthermore, Rg5 stimulated C2C12 myotube hypertrophy via phosphorylation of Akt/mTOR. Phosphorylation of Akt induces FoxO3a phosphorylation, which reduces the expression of Atrogin-1 and MuRF1.

Conclusion: This study provides an understanding of how Rg5 promotes myogenesis and hypertrophy and prevents dexamethasone-induced muscle atrophy. The study is the first, to the best of our knowledge, to show that Rg5 promotes muscle regeneration and to suggest that Rg5 can be used for therapeutic intervention of muscle weakness and atrophy, including cancer cachexia.

© 2023 The Korean Society of Ginseng. Publishing services by Elsevier B.V. This is an open access article under the CC BY-NC-ND license (<http://creativecommons.org/licenses/by-nc-nd/4.0/>).

* Corresponding author. Drug Information Research Institute, Muscle Physiome Research Center, College of Pharmacy, Sookmyung Women's University, Cheongpa-ro 47-gil 100, Yongsan, Seoul, 04310, Republic of Korea.

** Corresponding author. Research Institute of Aging Related Disease, AniMusCure Inc., Seobu-ro 2066, Jang-an, Suwon, 16419, Republic of Korea.

*** Corresponding author. Research Institute of Aging Related Disease, AniMusCure Inc., Seobu-ro 2066, Jang-an, Suwon, 16419, Republic of Korea.

E-mail addresses: ggy4428@animuscure.com (G.-Y. Go), animus_sjlee@animuscure.com (S.-J. Lee), gbae@sookmyung.ac.kr (G.-U. Bae).

¹ These authors contributed equally to this work.

1. Introduction

Approximately half of the human body weight consists of skeletal muscles. The skeletal muscles play a role not only in physical activity but also in glucose uptake and energy metabolism. Therefore, loss of skeletal muscle mass, known as muscle atrophy, leads to physical inactivity, obesity, and metabolic diseases [1,2]. Muscle atrophy is mainly caused by a decrease in myoblast differentiation or an imbalance between protein synthesis and decomposition [3–6].

Skeletal muscle differentiation (myogenesis) is a tightly regulated multistep process. It involves cell cycle exit, expression of muscle-specific proteins, and formation of multinucleated myotubes by cell fusion [7,8]. This process is coordinated by several

myogenic factors, such as myogenic determination gene number 1 (MyoD) and myogenic factor 5 (Myf5), which advance cells towards the myogenic lineage [9]. As differentiation progresses, the expression levels of muscle-specific proteins such as myogenin and myosin heavy chain (MHC) increase [8,10,11].

Myogenesis is activated by several signaling pathways. The p38 mitogen-activated protein kinase (p38MAPK) pathway, involved in myogenesis and activated by MKK6, regulates the activation of MyoD. Activation of MyoD is achieved by heterodimerization with the E proteins phosphorylated by p38MAPK [12]. In addition, p38MAPK induces cell cycle exit of myoblasts by regulating the activity of several chromatin remodeling proteins and antagonizing the c-Jun N-terminal kinase (JNK)/c-Jun pathway involved in the activation of myoblast cell cycle [11–14]. SB203580, a chemical that reduces the catalytic activity of p38MAPK by competitively inhibiting the ATP binding site, has been reported to inhibit differentiation and myotube fusion of C2C12 myoblasts [15].

The amount of muscle mass is determined by the equilibrium between protein synthesis and degradation [16]. When protein degradation overwhelms protein synthesis, muscle mass decreases. Therefore, studies on the promotion of protein synthesis and inhibition of protein degradation to alleviate muscular atrophy have been conducted. Among several anabolic signalings, the protein kinase B (Akt)/mammalian target of rapamycin (mTOR) signaling pathway is the representative protein synthetic pathway that plays a key role in skeletal muscle growth [17]. The Akt/mTOR pathway is activated by growth factors, amino acids, and intracellular energy status, leading to mTORC1 formation. Activated mTORC1 phosphorylates p70 S6 kinase 1 and eukaryotic initiation factor 4E-binding protein 1 (4EBP1), which promote protein translation by activating ribosomal protein S6 and releasing the eukaryotic translation initiation factor 4E (eIF-4E) [18,19]. According to previous studies, continuous activation of Akt results in muscle hypertrophy, with an increase in the cross-sectional area of muscle fibers [20,21]. Other studies have shown that the inactivation or absence of mTORC1 components and p70S6K1 in mouse skeletal muscles results in muscle mass loss [22–24].

Contrary to anabolic signaling, proteolytic systems, such as the ubiquitin-proteasome system (UPS) and autophagy-lysosome machinery, induce muscle loss. Activated forkhead box O3 (FoxO3) causes increased gene expression of muscle ring finger protein-1 (MuRF1), muscle atrophy F-box (MAFbx/Atrogin-1), and E3-ligases for muscle-specific protein degradation [20,25–27]. Since phosphoinositide 3-kinase (PI3K)/Akt signaling inhibits the activation of FoxO3, activating Akt signaling reduces UPS-mediated muscle atrophy [26–28]. Thus, the Akt/mTOR pathway increases muscle mass through the induction of protein synthesis along with the inhibition of the degradation of sarcomeric proteins such as MHC, troponins, and actin.

Since skeletal muscle is responsible for physical activity and energy and protein metabolism, various studies have reported that the quantity and function of skeletal muscles affect the lifespan and quality of life [29,30]. Therefore, researchers have made great efforts to increase muscle mass and regeneration capacity through studies to promote differentiation, increase protein synthesis, or inhibit degradation of muscle proteins. According to one study, testosterone, an androgen receptor ligand, induces Akt-induced muscle hypertrophy. Another study showed that neutralizing myostatin, a ligand of activin type II receptors (ActRIIa/b) that inhibits differentiation of myoblasts, or binding to the receptor in a competitive manner can alleviate delayed differentiation [31–33]. However, despite many studies being conducted, there is no drug till now that has passed clinical trials owing to hepatotoxicity and unpredictable prognosis.

Ginsenoside Rg5, a component of ginseng, is amplified by an iterative heating process [34,35], and it is more abundant in black ginseng than in unprocessed ginseng. Rg5 is a compound produced by the dehydration of Rg3, and it is known as the constitutional isomer of Rk1, which is a compound produced by the same process [36]. It has been reported to exhibit a broad range of pharmacological efficacy such as anti-neurological disorders and anti-inflammatory and anticancer effects [37–40]. However, studies on the evaluation of the effects of Rg5 on muscle differentiation and growth are scarce.

In this study, we analyzed the effects of Rg5, one of the major components of black ginseng, on muscle differentiation and growth. Rg5 promoted myogenesis through phosphorylation of p38MAPK and induced hypertrophy and prevented dexamethasone-induced atrophy through the Akt/mTOR signaling. Taken together, these findings suggest that Rg5 is a potential therapeutic agent to treat muscle weakness and atrophy.

2. Methods

2.1. Cell culture and isolation of primary myoblasts

A mouse myoblast cell line (C2C12) was obtained from ATCC (No. CRL-1772, Rockville, MD, USA). C2C12 myoblasts were cultured in Dulbecco's Modified Eagle Medium (DMEM)-high glucose (Gibco, Grand Island, NY, USA) supplemented with 15% fetal bovine serum (FBS; Gibco) and antibiotics (100 units/ml penicillin and 100 µl/ml streptomycin; Welgene, Gyeongsan-si, Gyeongsangbuk-do, South Korea). To induce differentiation of C2C12 cells at 80–90% confluency, the growth medium was replaced with differentiation medium [DMEM-high glucose (Gibco) supplemented with 2% horse serum (Gibco) and antibiotics (100 units/ml penicillin and 100 µl/ml streptomycin; Welgene)]. A human embryonic kidney cell line (HEK293T) was obtained from ATCC (No. CRL-3216). HEK293T cells were cultured in DMEM-high glucose (Gibco) supplemented with 10% FBS (Gibco) and antibiotics (100 units/ml penicillin and 100 µl/ml streptomycin; Welgene). For immunoprecipitation, HEK293T cells were transfected with MyoD (10 µg/100pi) and Lipofectamine 2000 (Thermo Fisher Scientific, Carlsbad, CA, USA). The cells were treated with Rg5 under different growth conditions. Primary myoblasts were isolated from the hindlimb muscles of 2–3-week-old mice. The muscles were isolated and digested with 1 mg/ml collagenase/dispase in phosphate-buffered saline (PBS). Isolated cells were cultured in growth medium containing 20% FBS (Gibco), 2.5 ng/ml basic fibroblast growth factor (Gibco), 10 ng/ml hepatocyte growth factor (Millipore, Billerica, MA, USA), and antibiotics (100 units/ml penicillin and 100 µl/ml streptomycin; Welgene). To induce differentiation of primary myoblasts, the growth medium was replaced with differentiation medium [DMEM-high glucose (Gibco) supplemented with 2% horse serum (Gibco) and antibiotics (100 units/ml penicillin and 100 µl/ml streptomycin; Welgene). The cells were maintained in a 37°C incubator with 5% CO₂ and 95% humidity.

2.2. Western blot analysis and immunoprecipitation

Cells were lysed using radioimmunoprecipitation assay (RIPA) buffer supplemented with 10 mM sodium fluoride, 1 mM sodium vanadate, and 1 × protease inhibitor (GenDEPOT, Katy, TX, USA) for protein extraction. Subsequently, SDS-PAGE and western blotting were performed. The primary antibodies used are listed in Table 1.

Western blotting was performed on immunoprecipitated samples. After protein extraction, anti-E2A antibody (1 µg) was added to the lysate (1 µg proteins) and incubated for 24 h at 4°C. Protein A agarose beads (Roche) were then added and incubated for 24 h at

Table 1
Antibodies.

Antibodies	Source	Catalog
MHC	DSHB	MF20 (hybridoma)
Myogenin	DSHB	IF05 (hybridoma)
MyoD	Santacruz	sc-32758
E2A	Santacruz	sc-133075
Phosphorylated p38	Cell signaling technology	4511
p38	Cell signaling technology	9212
Phosphorylated Akt	Cell signaling technology	4060
Akt	Cell signaling technology	9272
Phosphorylated mTOR	Cell signaling technology	5536
mTOR	Cell signaling technology	2983
Phosphorylated p70S6K	Cell signaling technology	9234
p70S6K	Santacruz	sc-2330
Atrogin-1	Santacruz	sc-166806
MuRF1	Santacruz	sc-398608
Pan-Cadherin	Santacruz	sc-59876
α -tubulin	Santacruz	sc-5286
HSP90	Santacruz	sc-13119
Alexa Fluor 488-linked anti-mouse IgG	Thermo Fisher	A28175
Alexa Fluor 555-linked anti-mouse IgG	Thermo Fisher	A28180

4°C. The complexes were then washed thrice with RIPA buffer. The samples were boiled with 2 × Laemmli sample buffer (Bio-Rad, Hercules, CA, USA) before analysis by western blotting.

2.3. Immunocytochemistry

Immunostaining was performed to visualize MHC expression levels. C2C12 cells or primary myoblasts were treated with the vehicle (dimethyl sulfoxide, DMSO), Rk1, or Rg5. The cells were fixed with 4% paraformaldehyde, permeabilized with 0.5% Triton X-100 in PBS, blocked, and stained with anti-MHC for 24 h at 4°C. The cells were then incubated with fluorescent-conjugated secondary antibody (Alexa Fluor 594), and images were acquired using Axio Observer Z1 LSM 700 (Zeiss).

2.4. Cell viability assay

MTT assay was used to determine cell viability. C2C12 cells were seeded in a 96-well plate and incubated for 24 h to allow attachment to the bottom of the plate. Rg5 was added at gradually increasing concentrations and incubated for 24 h. The cells were treated with 0.1 mg of MTT per well and incubated for 3 h to allow reduction of MTT. The cells were solubilized with 200 μ l DMSO, and the optical density was measured at 560 nm. The absorbance at the background wavelength of 670 nm was subtracted.

2.5. RNA extraction and quantitative RT-PCR

Total RNA was extracted from C2C12 cells using TRIzol reagent (Invitrogen, Carlsbad, CA, USA). cDNA was synthesized from RNA using the iScript Reverse Transcriptase (Bio-Rad). qRT-PCR analysis was performed with 2 × SYBR Green mix (MGmed, Seoul, South Korea). Each gene expression was normalized to glyceraldehyde-3-phosphate dehydrogenase (GAPDH) housekeeping gene expression. The primer sequences used are listed in Table 2.

2.6. Statistical analysis

Data or values mentioned in the figure legends are represented as either mean \pm standard deviation (SD) or standard error of the mean (SEM). For comparison between two groups, statistical significance was determined using an unpaired two-tailed Student's *t*-

test. For comparison between multiple groups, statistical significance was tested using one-way or two-way analysis of variance (ANOVA). Statistical significance was set at **P* < 0.05, ***P* < 0.01, and ****P* < 0.001.

3. Results

3.1. Treatment with ginsenoside Rg5 but not with Rk1 promotes myogenesis

Previous reports have shown that black ginseng enhances myogenesis [41–43]. Among various components of black ginseng, the amount of Rg5 and Rk1 is increased with the repetitive steaming and drying processes. Thus, we hypothesized that the myogenic effect of black ginseng was due to the presence of either Rg5 or Rk1 (Fig. 1A). To identify the effects of Rg5 and Rk1, C2C12 cells were subjected to differentiate with 100 nM Rg5 or Rk1. Next, we analyzed the expression levels of MHC and myogenin. The expression levels of MHC and myogenin were increased in Rg5-treated C2C12 cells, whereas no significant difference was observed between Rk1-treated and vehicle-treated cells (Fig. 1B). Based on immunostaining analysis of MHC, there were more multinucleated cells in Rg5-treated cells than those in vehicle (DMSO)-treated cells. However, Rk1-treated cells did not show any significant difference (Fig. 1C and D). Based on these results, we analyzed the phosphorylation level of p38MAPK, a representative signaling molecule related to myogenesis, and observed that the phosphorylation level of p38MAPK increased in Rg5-treated cells, but there was no significant change in Rk1-treated cells (Fig. 1E). Therefore, these data show that Rg5 has a myogenic effect, which might be associated with the phosphorylation of p38MAPK.

3.2. Treatment with ginsenoside Rg5 promotes myogenesis in a dose-dependent manner

After confirmation of the myogenic effect of Rg5, we conducted a series of experiments to examine whether this effect occurs in a dose-dependent manner and to determine the concentration of Rg5 that most efficiently elevates the expression of myogenic markers. Prior to this, we determined the effect of Rg5 on the viability of C2C12 cells. There was no significant change in cell viability within 0–3 μ M of Rg5 (Fig. 2A). Next, C2C12 cells were

Table 2
Primer Sequences.

Gene	Sequences	
	Forward	Reverse
MyoG	ATC TCC GCT ACA GAG GCG GG	TAG GGT CAG CCG CGA GCA AA
MyHC7	CCA TCT CTG ACA ACG CCT ATC	GGA TGA CCC TCT TAG TGT TGA C
MyHC2	AAG TGA CTG TGA AAA CAG AAG CA	GCA GCC ATT TGT AAG GGT TGA C
MyHC1	TTC ATT AGT TTC CCA GCT CTC C	AGC CAC TCT TGG CCT TTA TC
MyHC4	GAT TGA CGT GGA GAG GTC TAA C	CCT GAG TTT CCT CGT ACT TCT G
Atrogin-1	CAT GCG GTT CAA GCC ACT G	GTC TGG TTA CAC TTG GTG GAG
MuRF1	GAG TGG GTT TGG AGA CAA AGA	CCA GCA TGG AGA TGC AGT TA

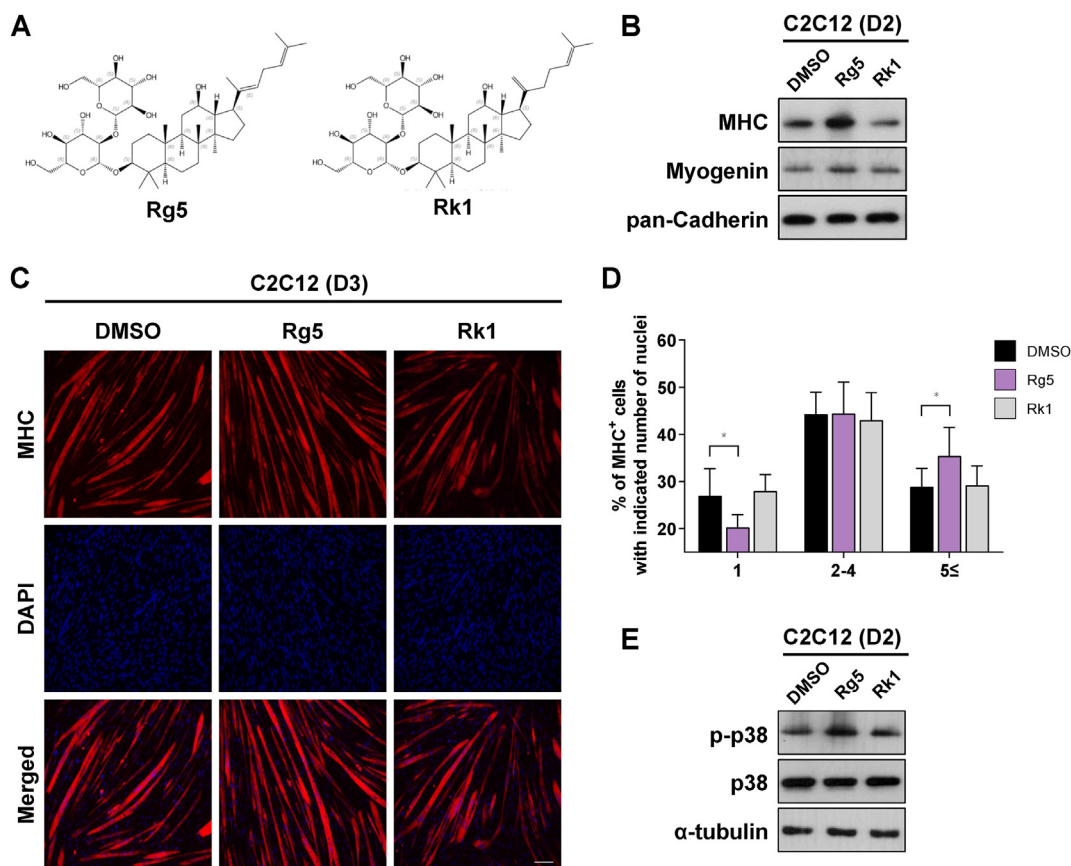
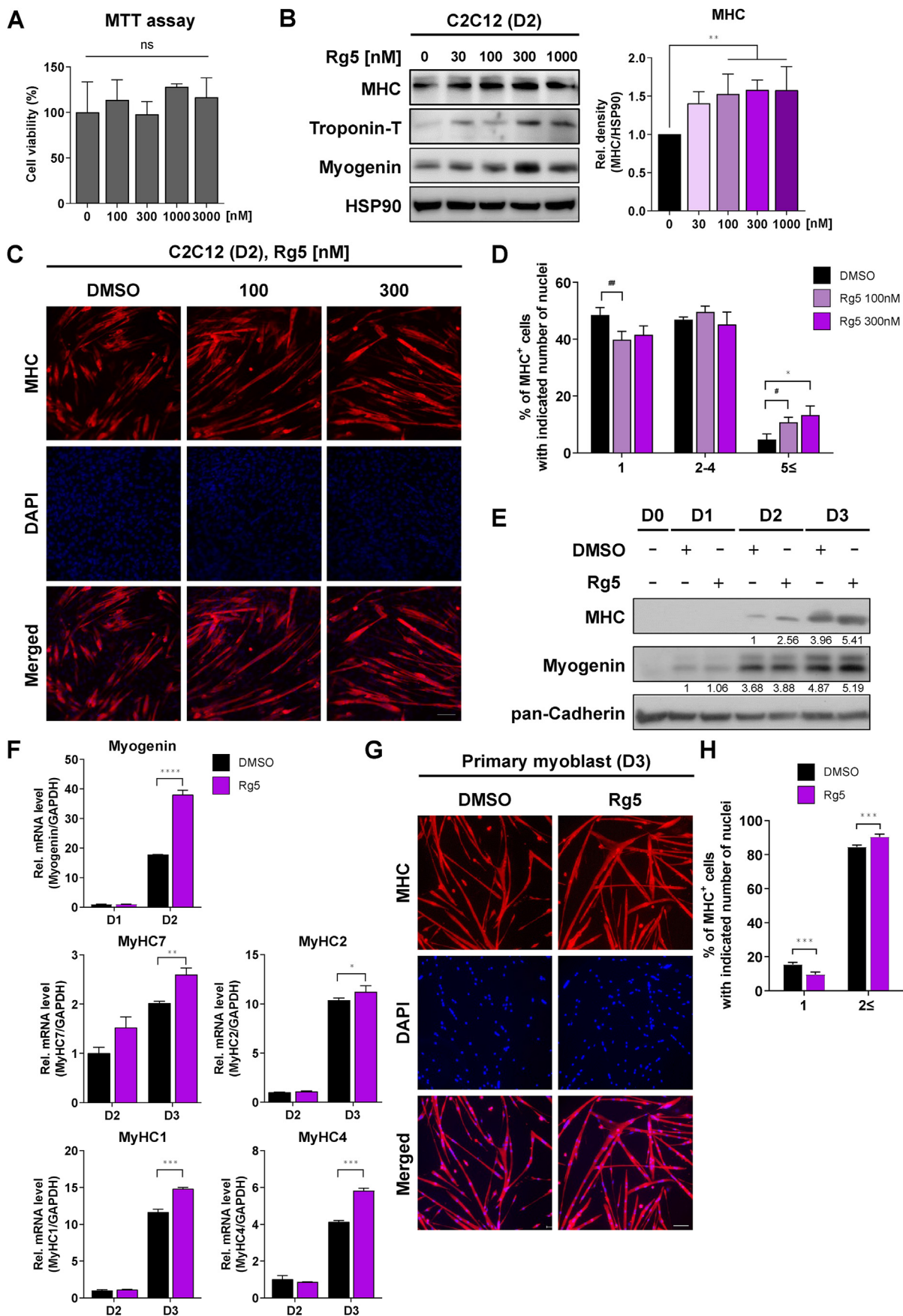


Fig. 1. Treatment with ginsenoside Rg5 but not with Rk1 promotes myogenesis (A) Structures of Rg5 and Rk1. (B) C2C12 cells that were induced to differentiate for 48 h (D2) in differentiation medium with 100 nM Rg5, Rk1, or vehicle (DMSO). The expression levels of the myogenic markers MHC and myogenin were analyzed by western blotting. (C) C2C12 cells were induced to differentiate for 72 h (D3) in differentiation medium with 100 nM Rg5, Rk1, or vehicle (DMSO), followed by immunostaining for MHC. Nuclei were visualized using DAPI staining (blue). Scale bar = 100 μ m (D) Quantification of immunostained C2C12 myotubes shown in Fig. 1C. Values represent the percentage of MHC-positive cells with the indicated number of nuclei and were calculated as the proportion of the number of multinucleated MHC-positive cells to the total number of MHC-positive cells (N = 4). Data represent the mean \pm SD. Statistical significance was determined using two-way ANOVA. *P < 0.05; Rg5 vs. vehicle (DMSO). (E) C2C12 cells that were maintained for 48 h (D2) in differentiation medium with 100 nM Rg5, Rk1, or vehicle (DMSO). Phosphorylated p38MAPK and p38MAPK expression levels were analyzed by western blotting. Pan-cadherin was used as a loading control.

cultured and treated with various concentrations of Rg5. The expression of MHC, troponin-T, and myogenin increased in a dose-dependent manner until 300 nM of Rg5. However, there was no proportional increase in the myogenic effect at 1 μ M (Fig. 2B). Therefore, we selected 300 nM as the optimal concentration, as it was the minimum concentration that showed the highest effect. Moreover, multinucleated myotubes containing ≥ 5 nuclei were significantly increased with Rg5 in a dose-dependent manner (Fig. 2C and D).

Subsequently, we investigated whether the effect of Rg5 was maintained during the overall differentiation. The expression levels of MHC and myogenin increased in Rg5-treated cells compared with those in the control group from day 2 to day 3. Additionally, treatment with Rg5 resulted in an increase in the mRNA expression of myogenin and subsequently in the expression levels of several isoforms of MyHC genes, which encode different MHC types (Fig. 2E and F).

Furthermore, we analyzed the myogenic effects of Rg5 on primary myoblasts, a robust system for studying muscle cells *ex vivo*.



We isolated primary myoblasts from the hindlimb muscles of mice aged 2–3 weeks and induced them to differentiate by treating them with Rg5. The results showed that the number of fused myoblasts was increased in Rg5-treated cells compared to that in the control group (Fig. 2G and H).

Taken together, Rg5 exhibits concentration-dependent myogenic effects, which is observed not only in C2C12 cells but also in primary myoblasts.

3.3. Rg5 promotes myogenesis through phosphorylation of Akt and p38MAPK

Phosphorylation of p38MAPK and subsequent activation of transcription factors promote myogenesis [12–14]. We investigated whether the myogenic effect of Rg5 is mediated by the phosphorylation of p38MAPK. The phosphorylation levels of p38MAPK gradually increased with Rg5 in a dose-dependent manner (Fig. 3A). In addition, we treated the cells with a p38MAPK inhibitor (SB203580) and Rg5 to determine whether the myogenic effect of Rg5 was inhibited by the blockade of p38MAPK. The expression levels of MHC and myogenin increased when Rg5 was used alone, whereas the expression levels decreased when the inhibitor was used, regardless of the presence of Rg5. These results indicate that the myogenic effect of Rg5 is associated with the p38MAPK pathway (Fig. 3B).

As mentioned earlier, the phosphorylation of p38MAPK induces myogenesis by increasing the binding of MyoD and E2A [12]. We performed immunoprecipitation to confirm whether p38MAPK phosphorylation via Rg5 increased the interaction between MyoD and E2A and observed that the interaction was increased after Rg5 treatment in both MyoD-transfected HEK293T and C2C12 cells (Fig. 3C and D).

These data show that the effect of Rg5 on myogenesis is associated with an increase in the phosphorylation levels of p38MAPK and an increase in MyoD activity.

3.4. Ginsenoside Rg5 treatment promotes hypertrophy through phosphorylation of Akt and attenuates dexamethasone-induced atrophy

Based on previous studies that demonstrated stimulation of muscle hypertrophy by black ginseng [41–43], we determined the effects of Rg5 on stimulating muscle hypertrophy and preventing muscle atrophy.

C2C12 myotubes were treated with Rg5 and dexamethasone. The expression of MHC increased with Rg5 treatment but decreased with dexamethasone treatment. However, co-treatment

with Rg5 and dexamethasone restored MHC expression (Fig. 4A). Additionally, immunostaining to visualize MHC expression levels was performed under the same conditions to confirm whether Rg5 could cause hypertrophy with an increase in the diameter of myotubes and prevent dexamethasone-induced atrophy. We observed an increase in the diameter of the myotubes in Rg5-treated myotubes but a decrease in the diameter in dexamethasone-treated myotubes. As expected, the diameter was restored in co-treated myotubes (Fig. 4B and C).

Next, we analyzed the effect of Rg5 on the Akt/mTOR pathway, a representative signaling pathway involved in protein synthesis. The overall phosphorylation levels of Akt, mTOR, and p70S6K were increased by Rg5 treatment but decreased by dexamethasone treatment. Moreover, co-treatment with Rg5 and dexamethasone restored the phosphorylation levels (Fig. 4D). Interestingly, protein expression and mRNA levels of Atrogin-1, MuRF1, and E3 ligases that break down muscle-specific proteins were reduced in co-treated myotubes compared with those in dexamethasone-treated myotubes (Fig. 4E and F).

These results confirm that Rg5 induces hypertrophy via the Akt/mTOR signaling pathway and prevents dexamethasone-induced atrophy.

4. Discussion

Despite endless research on skeletal muscles, there are no Food and Drug Administration (FDA)-approved drugs to improve muscle function and strength associated with pathological conditions or aging. Based on the study by Lee et al, who demonstrated stimulation of myogenesis by black ginseng extract [42], we performed screening to determine the constituent substances effective against muscle atrophy and identified Rg5 that exhibited myogenic effect. There are few studies on the effect of ginsenoside Rg5 in muscle metabolism [41,43]. However, there are no studies reported the myogenic and muscle growth effects of Rg5. Therefore, in this study, we investigated the potential of Rg5 as a therapeutic agent for muscle atrophy. Our data showed that Rg5 could help in the development and regeneration of muscles by promoting myogenesis through phosphorylation of p38MAPK, increasing protein synthesis through the Akt/mTOR signaling, and decreasing the expression of atrophy-related factors such as Atrogin-1 and MuRF1.

Ginsenosides Rg5 and Rk1 are constitutional isomers. 21C in Rg5 and 22C in Rk1 form a double bond with 20C, and no significant structural differences were observed between the two compounds (Fig. 1A). However, the two compounds possessed different myogenic effects (Fig. 1B–E). The arrangement of double bonds

Fig. 2. Treatment with ginsenoside Rg5 promotes myogenesis in a dose-dependent manner (A) MTT assay result of C2C12 cells treated with Rg5 (100, 300, 1000, or 3000 nM) or vehicle (DMSO). Cell viability was calculated as the proportion of absorbance value at 560 nm/670 nm to that of the vehicle. (B) C2C12 cells that were maintained for 48 h (D2) in differentiation medium with Rg5 (30, 100, 300, or 1000 nM) or vehicle (DMSO). The expression levels of the myogenic markers MHC, troponin-T, and myogenin were analyzed by western blotting. The MHC expression levels were normalized to HSP90 and were expressed as fold change values to that of the vehicle (DMSO). All values represent the mean \pm SEM of fold change values from three independent experiments. Statistical significance was determined using one-way ANOVA. * $P < 0.05$, ** $P < 0.01$; Rg5 vs. vehicle (DMSO). (C) C2C12 myotubes that were maintained for 48 h (D2) in differentiation medium with 100 or 300 nM of Rg5 or vehicle (DMSO), followed by immunostaining for MHC. Nuclei were visualized by DAPI staining (blue). Scale bar = 100 μ m. (D) Quantification of immunostained C2C12 myotubes shown in Fig. 2C. Values represent the percentage of MHC-positive cells with the indicated number of nuclei and were calculated as the proportion of the number of multinucleated MHC-positive cells to the total number of MHC-positive including mononucleated cells (N = 4). Data represent the mean \pm SD. Statistical significance was determined using two-way ANOVA. * $P < 0.05$; 300 nM Rg5 vs. vehicle (DMSO). ## $P < 0.01$, # $P < 0.05$; 100 nM Rg5 vs. vehicle (DMSO). (E) C2C12 cells were maintained for indicated days (D0–D3) with 300 nM Rg5 or vehicle (DMSO). The expression levels of the myogenic markers MHC and myogenin were analyzed by western blotting. Pan-Cadherin was used as a loading control. The MHC and myogenin expression levels were normalized to pan-Cadherin and were expressed as fold change values to those of the vehicle (DMSO). (F) C2C12 cells treated with 300 nM Rg5 or vehicle (DMSO) at 24 h (D1), 48 h (D2), and 72 h (D3). The relative mRNA expression levels of myogenin were expressed as fold change values to those of the vehicle (DMSO) at 24 h (D1). The relative mRNA expression levels of MyHC 7, 2, 1, and 4 were expressed as fold change values to those of the vehicle (DMSO) at 48 h (D2). The mRNA levels were normalized to the levels of GAPDH in the same samples. Values represent the mean \pm SEM. Statistical significance was determined using one-way ANOVA. * $P < 0.05$, ** $P < 0.01$, *** $P < 0.001$; Rg5 vs. vehicle (DMSO). (G) Primary myoblast cells were maintained for 72 h (D3) in a differentiation medium with 300 nM Rg5 or vehicle (DMSO), followed by immunostaining for MHC. Nuclei were visualized by DAPI staining (blue). Scale bar = 100 μ m. (H) Quantification of immunostained primary myoblast shown in panel of Fig. 2G. Values represent the percentage of MHC-positive cells with the indicated number of nuclei and were calculated as the proportion of the number of multinucleated MHC-positive cells to the total number of MHC-positive cells including mononucleated cells (N = 5). Data represent the mean \pm SD. Statistical significance was determined using two-way ANOVA. *** $P < 0.001$; Rg5 vs. vehicle (DMSO).

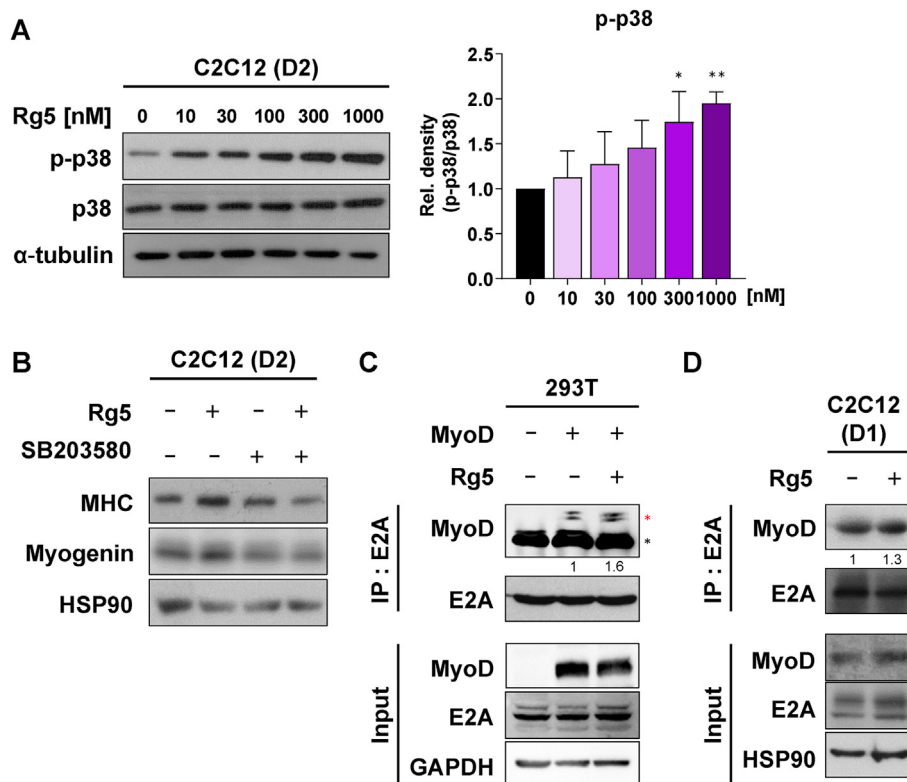


Fig. 3. Rg5 promotes myogenesis via phosphorylation of Akt and p38MAPK (A) C2C12 cells that were maintained for 48 h (D2) in differentiation medium with Rg5 (30, 100, 300, or 1000 nM) or vehicle (DMSO). The phosphorylation level of p38MAPK was analyzed by western blotting. The levels of phosphorylated p38MAPK were normalized to total p38MAPK and were expressed as fold change values to those of the vehicle (DMSO) group. All values represent the mean \pm SEM of fold change values from three independent experiments. Statistical significance was determined using one-way ANOVA. * $P < 0.05$, ** $P < 0.01$; Rg5 vs. vehicle (DMSO). (B) C2C12 cells that were maintained for 48 h (D2) in differentiation medium with Rg5 (300 nM), SB203580 (100 nM), or vehicle (DMSO). The expression levels of myogenic markers MHC and myogenin were analyzed by western blotting. HSP90 was used as a loading control. (C) MyoD-transfected HEK293T cells that were treated with Rg5 (300 nM) or vehicle (DMSO) for 24 h. The cell lysates were immunoprecipitated with E2A antibodies and blotted with MyoD and E2A antibodies. The red star represented MyoD bands and the black star represented IgG bands. Input represents an expression control. Quantification of the binding affinity of MyoD and E2A with Rg5 treatment, expressed as fold change relative to the vehicle (DMSO) treated control. (D) C2C12 cells that were maintained for 24 h (D1) in differentiation medium with Rg5 (300 nM) or vehicle (DMSO). The cell lysates were immunoprecipitated with E2A antibodies and blotted with MyoD and E2A antibodies. Input represents an expression control. Quantification of the binding affinity of MyoD and E2A with Rg5 treatment, expressed as fold change relative to the vehicle (DMSO) treated control.

may attribute to the different myogenic effects of the two ginsenosides.

Further, we confirmed that Rg5 promoted myogenesis through the phosphorylation of p38MAPK. In addition, Rg5 was treated with SB203580, a p38MAPK inhibitor, to determine whether Rg5 could promote myogenesis via pathways other than p38MAPK. The myogenic effect of Rg5 was inhibited after the blockade of p38MAPK, regardless of the presence of Rg5, indicating the major role of the p38MAPK pathway in the myogenic effect of Rg5 (Fig. 3B). Furthermore, we showed that Rg5 induced muscle hypertrophy through the Akt/mTOR signaling and inhibited glucocorticoid-induced atrophy. In this process, we induced the atrophy of C2C12 myotubes using dexamethasone, which is known to inhibit Akt phosphorylation [15,44]. The results demonstrated that Rg5 activated the Akt/mTOR signaling by competing with dexamethasone, resulting in the stimulation of muscle hypertrophy and inhibition of glucocorticoid-induced atrophy.

In muscles, FoxO3, a transcription factor, is activated by autophagic signals. Activation of FoxO3 increases the expression of atrogenes, such as Atrogin-1 and MuRF1, and has been reported to be inhibited by Akt [26]. Applying this to the dexamethasone-induced atrophy model, when the phosphorylation level of Akt was suppressed by dexamethasone, the activity of FoxO3 and expression of atrogenes increased. Therefore, we measured the expression of atrogenes to confirm that Rg5 treatment inhibited

dexamethasone-induced atrophy. The results revealed that the expression of atrogenes increased after dexamethasone administration but decreased after co-treatment with Rg5. The results indicated that the preventive effect of Rg5 on muscle atrophy was not only attributed to increased myogenic protein synthesis but also to the inactivation of FoxO3 which further affected the expression of atrogenes. However, studies using C2C12 cell lines and dexamethasone are not sufficient to reflect disease-induced muscle therapy. Consequently, it is necessary to validate these results through additional experiments and various models.

This study provides an understanding of how Rg5 promotes myogenesis and hypertrophy and prevents dexamethasone-induced muscle atrophy. Our data revealed that the myogenic effect of Rg5 was associated with the phosphorylation of p38MAPK. Previous studies have reported that phosphorylation of p38MAPK increases the interaction between E2A and MyoD. Therefore, we conducted immunoprecipitation to confirm the association between the myogenic effect of Rg5 and phosphorylation and increased interaction between E2A and MyoD. Furthermore, the results confirmed that Rg5 induced hypertrophy in C2C12 cells by increasing the diameter of myotubes and alleviating atrophy condition. These phenomena were found to be related to the activation or phosphorylation of the Akt/mTOR signaling. The study is the first, to the best of our knowledge, to show that Rg5 promotes muscle regeneration and to suggest that Rg5 can be used for

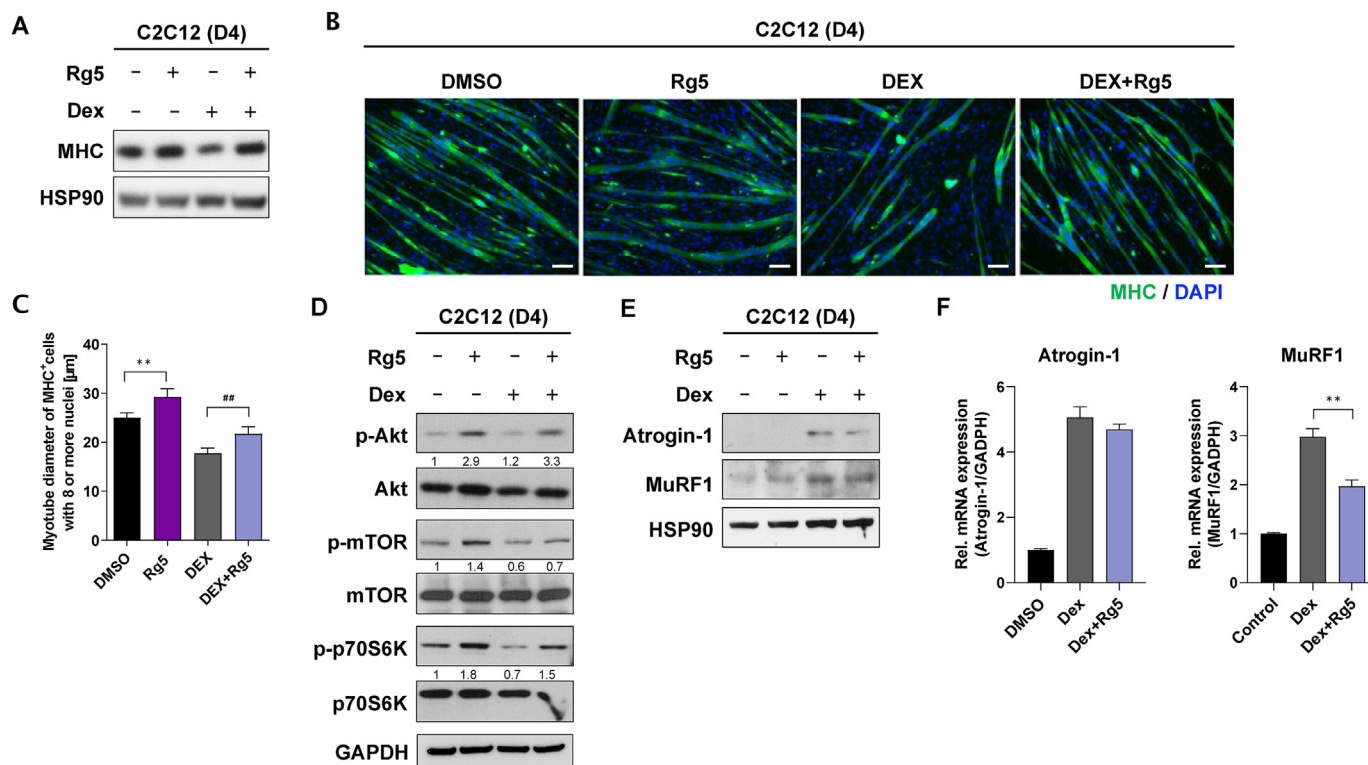


Fig. 4. Ginsenoside Rg5 treatment promotes muscle hypertrophy through phosphorylation of Akt and attenuates dexamethasone-induced atrophy. (A) C2C12 cells were maintained for 72 h in differentiation medium followed by treatment with dexamethasone (100 µM), Rg5 (300nM), or vehicle (DMSO) for 24 h. The expression of MHC was analyzed by western blotting. HSP90 was used as a loading control. (B) C2C12 cells were maintained for 72 h in differentiation medium followed by treatment with dexamethasone (100 µM), Rg5 (300nM), or vehicle (DMSO) for 24 h. MHC was targeted for immunostaining and Nuclei were visualized by DAPI (blue). Scale bar = 100µm. (C) Quantification of immunostained C2C12 myotubes diameter in Fig. 4B. Values represent the diameter of multinucleated MHC-positive cells with more than 8 nuclei (N = 4). Data were represented as the means ± SD. Statistical significance was determined by one-way ANOVA. **P < 0.01; Rg5 vs vehicle (DMSO). ##P < 0.01; DEX + Rg5 Vs DEX. (D) C2C12 cells were maintained for 72 h in differentiation medium followed by treatment with dexamethasone (100 µM), Rg5 (300nM), or vehicle (DMSO) for 24 h. Phosphorylation or total expression level of Akt, mTOR, and p70S6K was analyzed by western blotting. The phosphorylated levels of the proteins were normalized to the total expression levels of the proteins and expressed as fold change values to those of the vehicle (DMSO). (E) C2C12 cells were maintained for 72 h in differentiation medium followed by treatment with dexamethasone (100 µM), Rg5 (300nM), or vehicle (DMSO) for 24 h. The expression of Atrogin-1 and MuRF1 were analyzed by western blotting. HSP90 was used as a loading control. (F) C2C12 cells were maintained for 72 h in differentiation medium followed by treatment with dexamethasone (100 µM), Rg5 (300nM), or vehicle (DMSO) for 24 h. The relative mRNA expression level of Atrogin-1 and MuRF1 were calculated by the proportion of each expression level to the expression in the vehicle (DMSO). The mRNA levels were normalized to the levels of GAPDH in the same samples. Values are represented as means ± SEM. Statistical significance was determined by T-test. **P < 0.01; DEX + Rg5 vs DEX (DMSO).

therapeutic intervention of muscle weakness and atrophy, including cancer cachexia.

Declaration of competing interest

All authors have no conflicts of interest.

Acknowledgement

The present study was supported by the National Research Foundation of Korea (NRF) grant funded by the Korea government (MSIP; grant no. NRF-2021-COMPA-0101, NRF-2020-R1A2C1007555, NRF-2022-R1A5A2021216).

References

- [1] Perry BD, Caldwell MK, Brennan-Speranza TC, Sbaraglia M, Jerums G, Garnham A, Wong C, Levinger P, Asrar UI Haq M, Hare DL, et al. Muscle atrophy in patients with Type 2 Diabetes Mellitus: roles of inflammatory pathways, physical activity and exercise. *Exerc Immunol Rev* 2016;22: 94–109.
- [2] Wang M, Tan Y, Shi Y, Wang X, Liao Z, Wei P. Diabetes and sarcopenic obesity: pathogenesis, diagnosis, and treatments. *Front Endocrinol* 2020;11:568.
- [3] Domingues-Faria C, Vasson M-P, Goncalves-Mendes N, Boirie Y, Walrand S. Skeletal muscle regeneration and impact of aging and nutrition. *Ageing Res Rev* 2016;26:22–36.

- [4] Jagoe RT, Goldberg AL. What do we really know about the ubiquitin-proteasome pathway in muscle atrophy? *Curr Opin Clin Nutr Metab Care* 2001;4(3):183–90.
- [5] Larsson L, Degens H, Li M, Salvati L, Lee YI, Thompson W, Kirkland JL, Sandri M. Sarcopenia: aging-related loss of muscle mass and function. *Physiol Rev* 2019;99(1):427–511.
- [6] McKenna CF, Fry CS. Altered satellite cell dynamics accompany skeletal muscle atrophy during chronic illness, disuse, and aging. *Curr Opin Clin Nutr Metab Care* 2017;20(6):447–52.
- [7] Das M, Wilson K, Molnar P, Hickman JJ. Differentiation of skeletal muscle and integration of myotubes with silicon microstructures using serum-free medium and a synthetic silane substrate. *Nat Protoc* 2007;2(7):1795–801.
- [8] Molkenin JD, Olson EN. Defining the regulatory networks for muscle development. *Curr Opin Genet Dev* 1996;6(4):445–53.
- [9] Wardle FC. Master control: transcriptional regulation of mammalian MyoD. *J Muscle Res Cell Motil* 2019;40(2):211–26.
- [10] Braun T, Gautel M. Transcriptional mechanisms regulating skeletal muscle differentiation, growth and homeostasis. *Nat. Rev Mol Cell Biol* 2011;12(6): 349–61.
- [11] Yagi M, Ji F, Charlton J, Cristea S, Messemer K, Horwitz N, Di Stefano B, Tsopoulidis N, Hoetker MS, Huebner AJ, et al. Dissecting dual roles of MyoD during lineage conversion to mature myocytes and myogenic stem cells. *Genes Dev* 2021;35(17–18):1209–28.
- [12] Lluís F, Ballestar E, Suelves M, Esteller M, Muñoz-Cánoves P. E47 phosphorylation by p38 MAPK promotes MyoD/E47 association and muscle-specific gene transcription. *EMBO J* 2005;24(5):974–84.
- [13] Perdiguero E, Ruiz-Bonilla V, Gresh L, Hui L, Ballestar E, Sousa-Victor P, Baeza-Raja B, Jardí M, Bosch-Comas A, Esteller M, et al. Genetic analysis of p38 MAPK kinases in myogenesis: fundamental role of p38alpha in abrogating myoblast proliferation. *EMBO J* 2007;26(5):1245–56.

- [14] Serra C, Palacios D, Mozzetta C, Forcales SV, Morante I, Ripani M, Jones DR, Du K, Jhala US, Simone C, et al. Functional interdependence at the chromatin level between the MKK6/p38 and IGF1/PI3K/AKT pathways during muscle differentiation. *Mol Cell* 2007;28(2):200–13.
- [15] Xie Y, Perry BD, Espinoza D, Zhang P, Price SR. Glucocorticoid-induced CREB activation and myostatin expression in C2C12 myotubes involves phosphodiesterase-3/4 signaling. *Biochem Biophys Res Commun* 2018;503(3):1409–14.
- [16] Liguori I, Russo G, Aran L, Bulli G, Curcio F, Della-Morte D, Gargiulo G, Testa G, Cacciatore F, Bonaduce D, et al. Sarcopenia: assessment of disease burden and strategies to improve outcomes. *Clin Interv Aging* 2018;13:913–27.
- [17] Sandri M. Signaling in muscle atrophy and hypertrophy. *Physiol (Bethesda, Md)* 2008;23:160–70.
- [18] Kim DH, Sarbassov DD, Ali SM, Latek RR, Guntur KV, Erdjument-Bromage H, Tempst P, Sabatini DM. GbetaL, a positive regulator of the rapamycin-sensitive pathway required for the nutrient-sensitive interaction between raptor and mTOR. *Mol Cell* 2003;11(4):895–904.
- [19] Matsumoto A, Pasut A, Matsumoto M, Yamashita R, Fung J, Monteleone E, Saghatelian A, Nakayama KI, Cloughesy JG, Pandolfi PP. mTORC1 and muscle regeneration are regulated by the LINC00961-encoded SPAR polypeptide. *Nature* 2017;541(7636):228–32.
- [20] Bodine SC, Latres E, Baumhueter S, Lai VK, Nunez L, Clarke BA, Poueymirou WT, Panaro FJ, Na E, Dharmarajan K, et al. Identification of ubiquitin ligases required for skeletal muscle atrophy. *Sci (New York, NY)* 2001;294(5547):1704–8.
- [21] Lai K-MV, Gonzalez M, Poueymirou WT, Kline WO, Na E, Zlotchenko E, Stitt TN, Economides AN, Yancopoulos GD, Glass DJ. Conditional activation of at in adult skeletal muscle induces rapid hypertrophy. *Mol Cell Biol* 2004;24(21):9295–304.
- [22] Bentzinger CF, Romanino K, Cloëtta D, Lin S, Mascarenhas JB, Oliveri F, Xia J, Casanova E, Costa CF, Brink M, et al. Skeletal muscle-specific ablation of raptor, but not of rictor, causes metabolic changes and results in muscle dystrophy. *Cell Metabol* 2008;8(5):411–24.
- [23] Marabita M, Baraldo M, Solagna F, Judith Johanna Ceelen, Sartori R, Nolte H, Nemazany I, Pyronnet S, Kruger M, Pende M, et al. S6K1 is required for increasing skeletal muscle force during hypertrophy. *Cell Reports* 2016;17(2):501–13.
- [24] Risson V, Mazelin L, Roceri M, Sanchez H, Moncollin V, Corneloup C, Richard-Bulteau H, Vignaud A, Baas D, Defour A, et al. Muscle inactivation of mTOR causes metabolic and dystrophin defects leading to severe myopathy. *J Cell Biol* 2009;187(6):859–74.
- [25] Lecker SH, Goldberg AL, Mitch WE. Protein degradation by the ubiquitin-proteasome pathway in normal and disease states. *J Am Soc Nephrol: JASN*. 2006;17(7):1807–19.
- [26] Mammucari C, Milan G, Romanello V, Masiero E, Rudolf R, Del Piccolo P, Burden SJ, Di Lisi R, Sandri C, Zhao J, et al. FoxO3 controls autophagy in skeletal muscle in vivo. *Cell Metabol* 2007;6(6):458–71.
- [27] Sandri M, Sandri C, Gilbert A, Skurk C, Calabria E, Picard A, Walsh K, Schiaffino S, Lecker SH, Goldberg AL. Foxo transcription factors induce the atrophy-related ubiquitin ligase atrogin-1 and cause skeletal muscle atrophy. *Cell* 2004;117(3):399–412.
- [28] Stitt TN, Drujan D, Clarke BA, Panaro F, Timofeyeva Y, Kline WO, Gonzalez M, Yancopoulos GD, Glass DJ. The IGF-1/PI3K/akt pathway prevents expression of muscle atrophy-induced ubiquitin ligases by inhibiting FOXO transcription factors. *Mol Cell* 2004;14(3):395–403.
- [29] Demontis F, Piccirillo R, Goldberg AL, Perrimon N. The influence of skeletal muscle on systemic aging and lifespan. *Aging Cell* 2013;12(6):943–9.
- [30] Srikanthan P, Karlamangla AS. Muscle mass index as a predictor of longevity in older adults. *Am J Med* 2014;127(6):547–53.
- [31] Hughes DC, Stewart CE, Sculthorpe N, Dugdale HF, Yousefian F, Lewis MP, Sharples AP. Testosterone enables growth and hypertrophy in fusion impaired myoblasts that display myotube atrophy: deciphering the role of androgen and IGF-I receptors. *Biogerontology* 2016;17(3):619–39.
- [32] Morvan F, Rondeau J-M, Zou C, Minetti G, Scheufler C, Scharenberg M, Jacobi C, Brebbia P, Ritter V, Toussaint G, et al. Blockade of activin type II receptors with a dual anti-ActRIIA/IIb antibody is critical to promote maximal skeletal muscle hypertrophy. *Proc Natl Acad Sci* 2017;114(47):12448.
- [33] Suh J, Lee Y-S. Myostatin inhibitors: panacea or predicament for musculoskeletal disorders? *J Bone Metab* 2020;27(3):151–65.
- [34] Cho HT, Kim JH, Lee JH, Kim YJ. Effects of Panax ginseng extracts prepared at different steaming times on thermogenesis in rats. *J Ginseng Res* 2017;41(3):347–52.
- [35] Chu C, Xu S, Li X, Yan J, Liu L. Profiling the ginsenosides of three ginseng products by lc-Q-Tof/ms. *J Food Sci* 2013;78(5):C653–9.
- [36] Piao XM, Huo Y, Kang JP, Mathiyalagan R, Zhang H, Yang DU, Kim M, Yang DC, Kang SC, Wang YP. Diversity of ginsenoside profiles produced by various processing technologies. *Molecules* 2020;25(19).
- [37] Ahn S, Siddiqi MH, Aceituno VC, Simu SY, Zhang J, Jimenez Perez ZE, Kim YJ, Yang DC. Ginsenoside Rg5:Rk1 attenuates TNF- α /IFN- γ -induced production of thymus- and activation-regulated chemokine (TARC/CCL17) and LPS-induced NO production via downregulation of NF- κ B/p38 MAPK/STAT1 signaling in human keratinocytes and macrophages. *In Vitro Cellular Dev Biol Animal* 2016;52(3):287–95.
- [38] Choi SY, Kim KJ, Song JH, Lee BY. Ginsenoside Rg5 prevents apoptosis by modulating heme-oxygenase-1/nuclear factor E2-related factor 2 signaling and alters the expression of cognitive impairment-associated genes in thermal stress-exposed HT22 cells. *J Ginseng Res* 2018;42(2):225–8.
- [39] Kim H, Choi P, Kim T, Kim Y, Song BG, Park YT, Choi SJ, Yoon CH, Lim WC, Ko H, et al. Ginsenosides Rk1 and Rg5 inhibit transforming growth factor- β 1-induced epithelial-mesenchymal transition and suppress migration, invasion, anoikis resistance, and development of stem-like features in lung cancer. *J Ginseng Res* 2021;45(1):134–48.
- [40] Lee YY, Park JS, Jung JS, Kim DH, Kim HS. Anti-inflammatory effect of ginsenoside Rg5 in lipopolysaccharide-stimulated BV2 microglial cells. *Int J Mol Sci* 2013;14(5):9820–33.
- [41] Jeong YJ, Hwang MJ, Hong CO, Yoo DS, Kim JS, Kim DY, Lee KW. Anti-hyperglycemic and hypolipidemic effects of black ginseng extract containing increased Rh4, Rg5, and Rk1 content in muscle and liver of type 2 diabetic db/db mice. *Food Sci Biotechnol* 2020;29(8):1101–12.
- [42] Lee S-Y, Go G-Y, Vuong TA, Kim JW, Lee S, Jo A, An JM, Kim S-N, Seo D-W, Kim J-S, et al. Black ginseng activates Akt signaling, thereby enhancing myoblast differentiation and myotube growth. *J Ginseng Res* 2018;42(1):116–21.
- [43] Seo YS, Shon MY, Kong R, Kang OH, Zhou T, Kim DY, Kwon DY. Black ginseng extract exerts anti-hyperglycemic effect via modulation of glucose metabolism in liver and muscle. *J Ethnopharmacol* 2016;190:231–40.
- [44] Andrade M, Hiragun T, Beaven M. Dexamethasone suppresses antigen-induced activation of phosphatidylinositol 3-kinase and downstream responses in mast cells. *J Immunol (Baltimore, Md : 1950)* 2004;172:7254–62.